International Global Navigation Satellite Systems Society
IGNSS Symposium 2007

The University of New South Wales, Sydney, Australia
4 – 6 December, 2007

Evaluating the Performance of Low-Cost Inertial Sensors for use in Integrated Positioning Systems

Bing Li (1)
PhD Student/ The University of Melbourne/ Australia
+ 61 3 83440193 (O), + 61 3 83444616 (F), bingl@civenv.unimelb.edu.au

Allison Kealy (2)
Dr./ The University of Melbourne/ Australia
+ 61 3 83444616 (F), a.kealy@unimelb.edu.au

Colin F. Duffield (3)
Associate Professor/ The University of Melbourne/ Australia
+ 61 3 83444616 (F), colinfd@unimelb.edu.au

Graham L. Hutchinson (4)
Professor/ The University of Melbourne/ Australia
+ 61 3 83444616 (F), grahamlh@unimelb.edu.au

ABSTRACT

Over the past decade inertial sensor technologies have undergone a significant evolution with regards to their size, weight, power consumption and cost. What is still relatively undefined is the potential of these 'new' devices to augment GNSS performance. This task is essential given the growing number of applications that rely on position solutions, combined with an increasing range of positioning accuracy and reliability requirements. This paper presents results obtained from an extensive study undertaken to characterise the performance of current generation inertial sensors. A range of commercially available, low-cost inertial sensors were rigorously evaluated both statically and dynamically. This paper presents a description of the software tool developed to capture the data from all sensors simultaneously and the test platform designed to evaluate the performance of the sensors. A detailed description of the tests performed and the results obtained is also documented in this paper.

KEYWORDS: inertial sensors, MEMS technology, integrated positioning

1. INTRODUCTION

Global Navigation Satellite Systems (GNSS) are currently recognised as the primary technology for the majority of positioning and navigation application. However, while an ever increasing and diverse user community accepts that (under ideal conditions) GNSS can easily achieve the level of performance required, it also widely acknowledges that in certain environments the system can become highly unreliable. Obstructions including tree foliage and buildings impede signals as they travel from the satellites to the receiver, leaving insufficient measurements for positional computations. In addition, where signals do reach the receiver, they may have undergone reflections off surfaces before being received by the GNSS antenna. Such multipathing leads to unknown biases in the satellite-receiver range measurements. And this is simply a fundamental operating constraint of any microwave satellite system (McLellan, 1992).

The all-pervasive influence of GPS has established a trend in international research towards the integration of complementary technologies to remove this constraint, thereby expanding the capabilities of the system. In the majority of cases, the integration philosophy revolves around the augmentation of GPS measurements with dead reckoning (DR) or inertial (INS) systems, using Kalman filtering theory (Cannon et al, 1992). Whilst these systems offer some improvement in the performance of GPS during periods of complete or partial satellite obstruction, in all cases there are practical and theoretical constraints that have hindered their successful implementation.

This paper addresses the practical limitation facing integrated positioning systems in that *the precision of the solution obtained is dependent on the precision of the measurements obtained from the augmentation sensors.* Many engineering applications require continuous position solutions with centimetre level performance. The rapid accumulation of errors in low cost INS and the significantly high cost of more precise inertial sensors have precluded their use in the development of practical integrated solutions for these applications. This research has been inspired by recent progress in surface micromaching technologies, which has facilitated the development of MEMS inertial sensors (DARPA, 2007; Allen et al, 1998). For high precision applications, these developments are significant, as MEMS technologies are now enabling new form factors for inertial sensors. For example, the AGNC–2000 CMIMU™ inertial measurement unit has a volume of less than 16 cubic centimetres and weighs less than 28g. At this stage MEMS technology is still very immature and currently available sensors can only achieve tactical and low-end navigational grade accuracies. However, Sheimy (2000) has indicated that the current trend is towards the rapid development of higher performance MEMS instruments. Combined with cost reductions from tens of thousands of US dollars, e.g. Boeing C-MIGITS™ and Litton LN100™, to only tens of dollars e.g. Analogue Device ADXL202™ and AGNC–2000 CMIMU™, the potential of MEMS for improving GPS performance must be investigated. This research takes advantage of the exciting new platform offered by MEMS, to conduct innovative research into integrated positioning systems.

This paper presents a description of the data capture software, the testing strategy and preliminary results obtained from a range of experiments designed to characterise the performance of a range of commercially available MEMS sensors. A performance assessment of these sensors and their use in engineering structural monitoring activities is also presented.

2. METHOD

2.1 MEMS Sensors

Table 1 presents a summary of the characteristics of the 4 different MEMS sensors used in this study. These represent the range of commercially available sensors available today. They are Microstrain Inertia-Link™, Crossbow TG™, XSens MTi™, and Cloudcap Crista_IMU (Figure 1). Key design features of these sensors as stated by the manufacturers are listed in Table 1, from which some comparisons can be drawn:

- All the sensors are designed as tri-axial measurement devices.
- With the exception of sensor #2, all others are capable of measuring both tri-axial accelerations and tri-axial gyros.
- According to the specification sheets, all the sensors are designed to be precision instruments with low noise rates.
- Physically, all the sensors are small and light-weight

No	Sensor	Measurement	Range	Error	Sampling Rate	Noise	Size	Weight
1	Crista_IMU	3- Axial Acceleration	±10g	<1%	>1KHz		2.05"× 1.55" ×1.00"	36.8g
		3- Axial Gyros	±300° /sec	<1%				
2	Crossbow TG	3- Axial Acceleration	±2g	±0.0085g	> 200Hz	0.6mg rms	0.98"× 2.235" × 1.435"	110g
3	X-Sens MTi	3- Axial Acceleration	<2g	0.02 m/s2	512Hz	0.001 m/s2/ √Hz	58mm× 58mm× 22mm	50g
		3- Axial Gyros	±300° /sec	5 °/sec	120Hz	0.1 °/sec/√Hz		
4	Inertia Link	3- Axial Acceleration	±5g	±0.005g	1~250Hz		41mm× 63mm× 24mm	39g
		3- Axial Gyros	360°	±0.5° (S) ±2.0° (D)				

Table 1: Summary of Key Features of Sensors (From specification sheets)

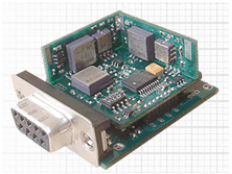

#1 Crista_IMU

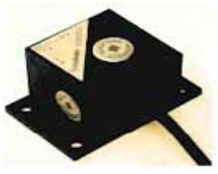

#2 Crossbow_TG

#3 X-Sens MTi

#4 Inertia Link

Figure 1: MEMS sensors

2.2 Design of Sensor Testing

Both static and dynamic tests have been designed and conducted specially for the purpose of evaluating the performance of sensors. This study will focus on three typical standards of sensors performances: repeatability, accuracy, and precision.

To capture the data from the sensors, a data logging software was developed for this research. The Universal Data Logger (UDL) enables all data to be captured simultaneously from all sensors connected to the computer via serial port and USB ports. The sensors are time tagged using either the pulse per second output from a GNSS receiver or with computer time. Figure 2 shows a screen capture from the UDL software. The UDL software also allows the user to specify the output format of the incoming data and to decode the binary data streams if necessary. The measurement data from the sensors are then logged to a Microsoft AccessTM database file for subsequent analysis.

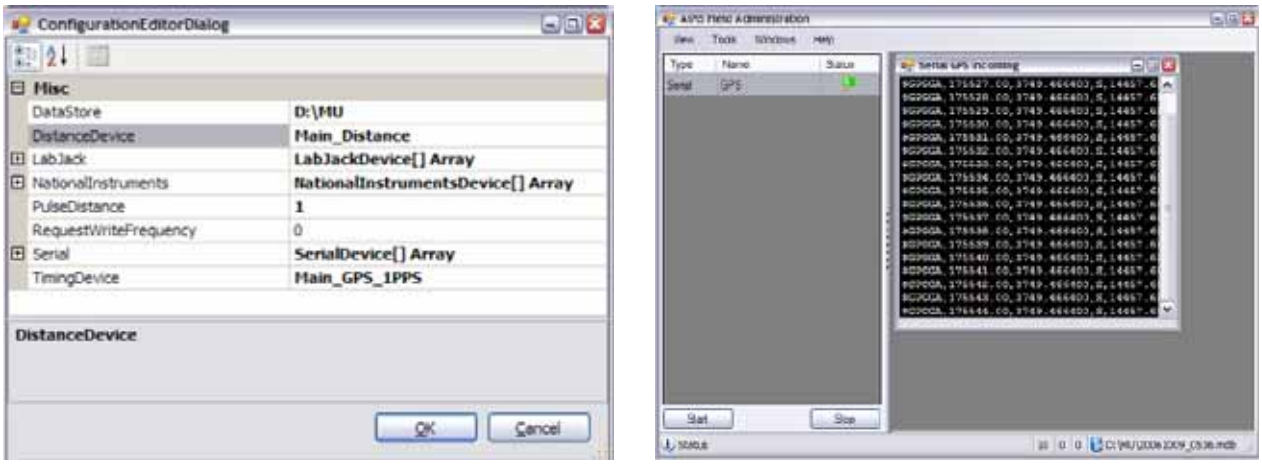

(a) (b)

Figure 2: Screen print of the Universal Data Logger software

2.2.1 Static test

Sensors No.1 to No.4 were attached to the test-bed which is a platform fixing to the structural wall of the laboratory. Relatively long measuring period (>24 hours) was designated so that the reliability of the sensors on long-term measurement can be fully validated. Moreover, the test has been repeated three times in order to verify the repeatability of the sensors.

Figure 3 shows the arrangement for static test. The static tests were conducted in a separate lab with restrictions on access of irrelevant people in order to reduce the outside excitation/ interruption and simulate static testing environment. However, vibrations of the building itself and some of the interruptions from mid-night cleaning activities were unable to be avoided.

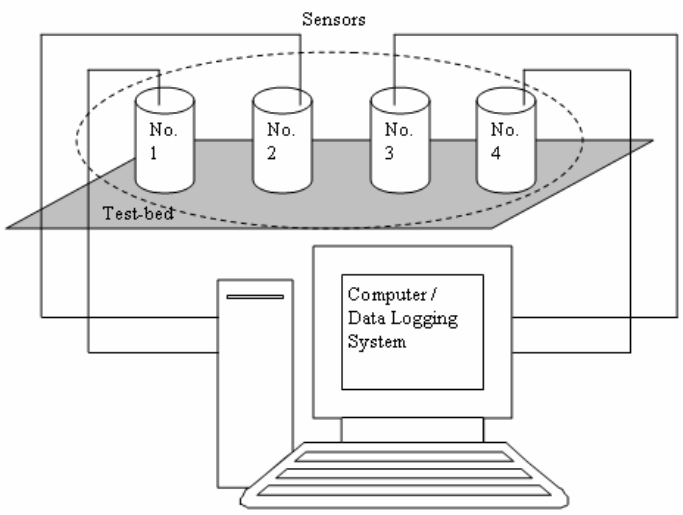

Figure 3: Arrangement of Static Test

2.2.2 Vibration test (Figure 4)

The vibration test was carried out in a structural laboratory by using Tinius machine which can provide constant and controllable vibrations as inputs. Simultaneously, two precise uniaxial accelerometers, Dytran 3191A and 3192A were also used as benchmarks to evaluate the target sensors. Only sensors No.2 and No.4 were tested and No.1 and No.3 were excluded in the test because of the impractical cable lengths and power supply.

During the vibration test, two computing/ data logging systems were involved because of the incompatibility of the two sets of data logging software. Moreover, since the Tinius machine is motivated by hydraulic pressure from the prestored mechanical oil, certain level of instability of the machine performance should be expected.

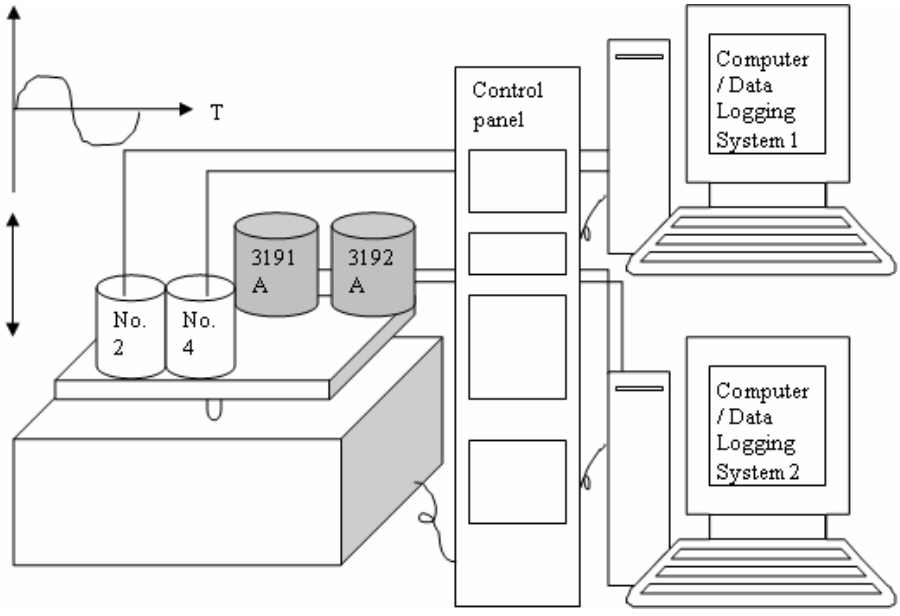

Figure 4: Arrangement of Vibration Test

2.2.3 Assumptions & scope/ limitations of designed tests

Constrained by the testing environment and the resources, there are some limitations and assumptions involved with the tests.

- Restrained by the static testing environment, the tests conducted should be semi-static tests. However, for the purpose of this paper, those results were considered as static testing results.

- Failure of synchronization of the two data logging system induced time lag between sensors. When doing data analysis, the lags were ignored and only key dynamic features of the data (frequency/ period and amplitude, etc.) were analysed and discussed.

3. RESULTS

3.1 Static Test

Possibility density function analysis results for sensors No.1 to 4 are shown in Figure 5 to Figure 16, accompanied by the plotted acceleration-time histories. Error range advertised by each manufacturer was also marked by dashed red lines. Maximum, minimum, and average readings of tri-axial accelerations are extracted from the every-second data and then analysed. To show the measurement clearly, results for three axes were plotted separately.

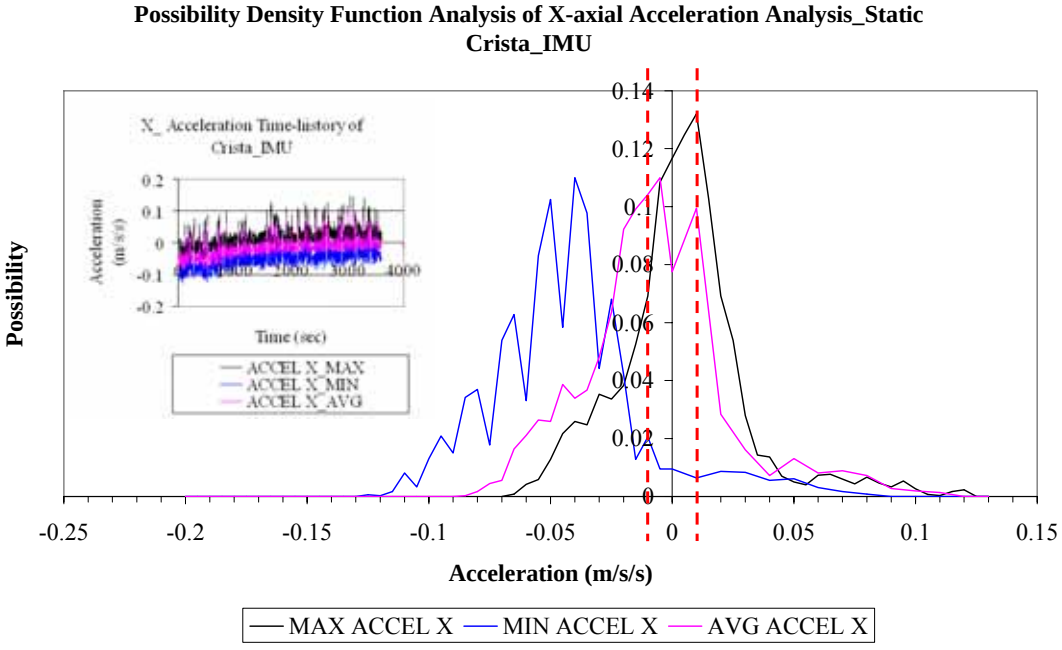

Figure 5: Possibility Density Function Analysis of X-Acceleration_Crista_IMU (Static)

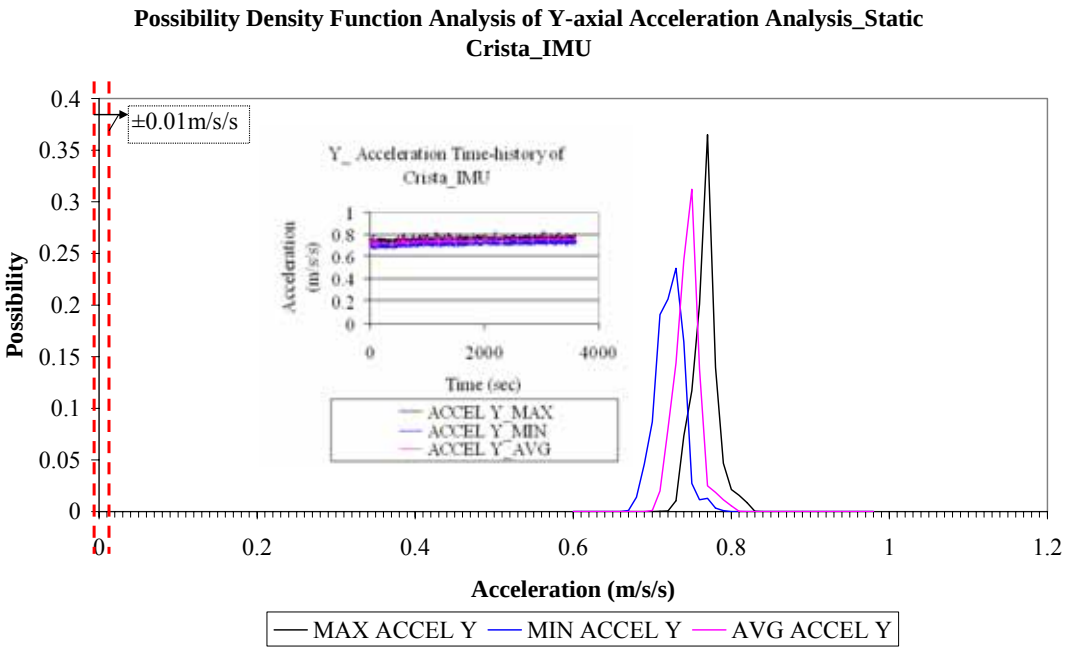

Figure 6: Possibility Density Function Analysis of Y-Acceleration_Crista_IMU (Static)

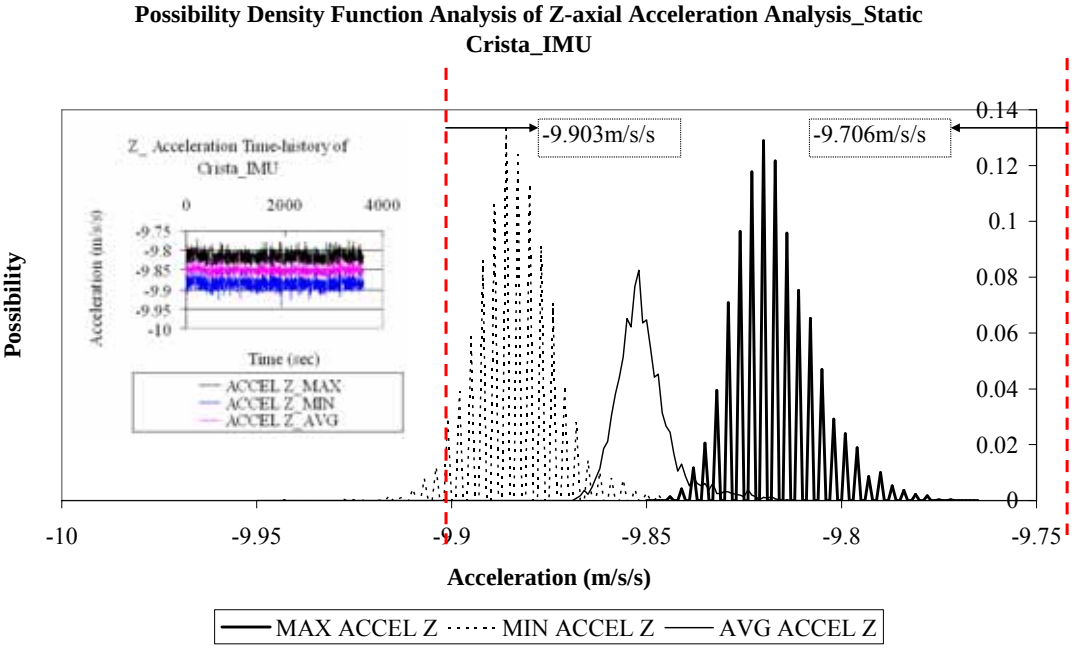

Figure 7: Possibility Density Function Analysis of Z-Acceleration_Crista_IMU (Static)

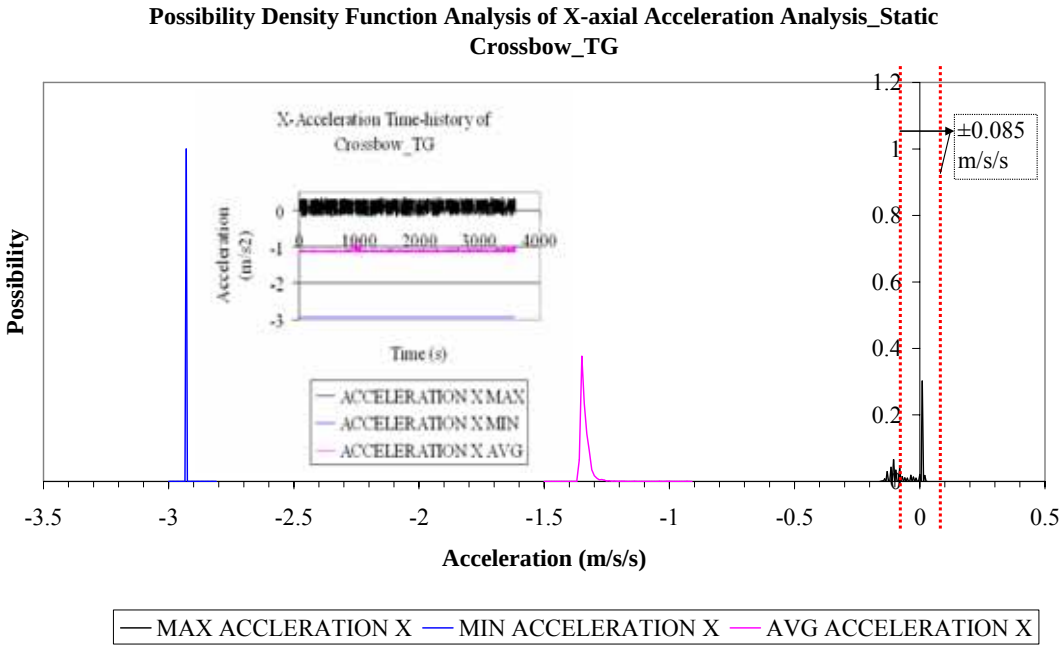

Figure 8: Possibility Density Function Analysis of X-Acceleration_Crossbow_TG (Static)

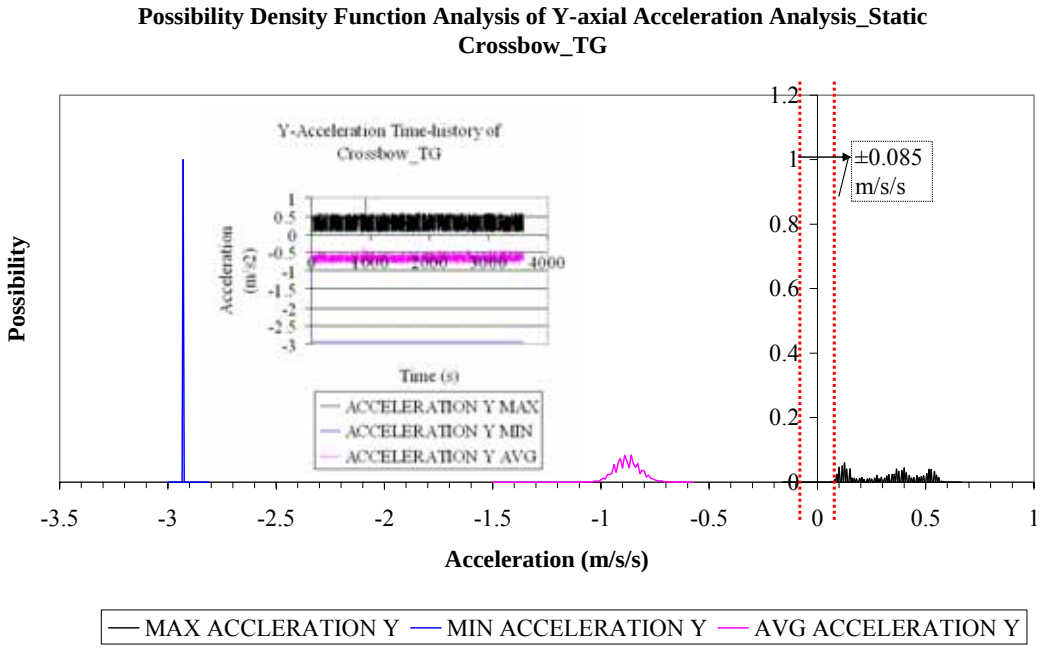

Figure 9: Possibility Density Function Analysis of Y-Acceleration_Crossbow_TG (Static)

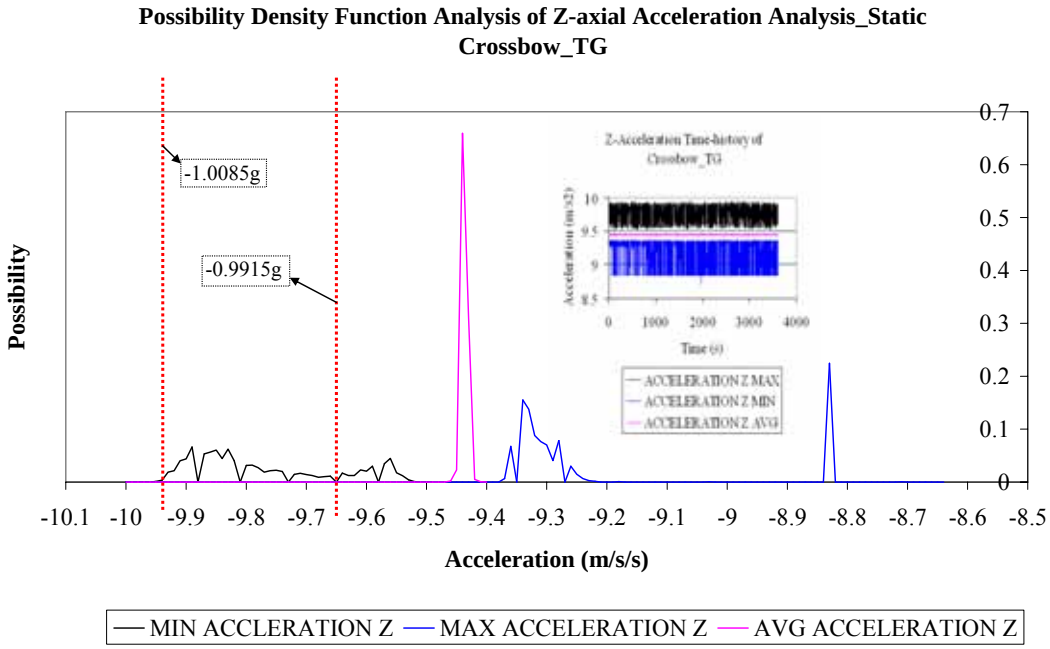

Figure 10: Possibility Density Function Analysis of Z-Acceleration_Crossbow_TG (Static)

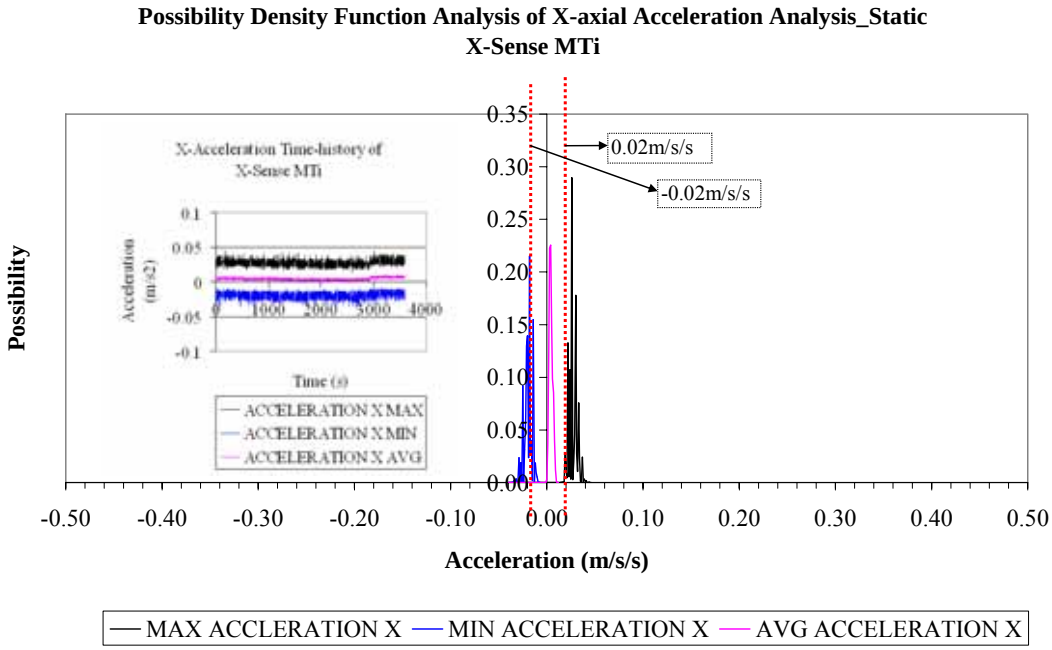

Figure 11: Possibility Density Function Analysis of X-Acceleration_MTi (Static)

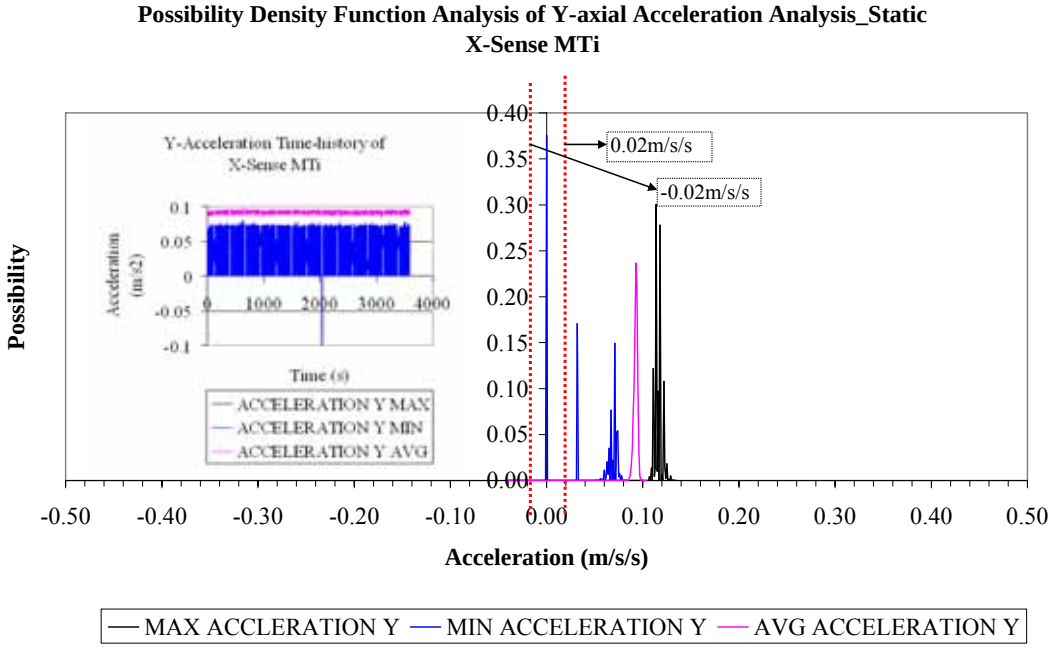

Figure 12: Possibility Density Function Analysis of Y-Acceleration_MTi (Static)

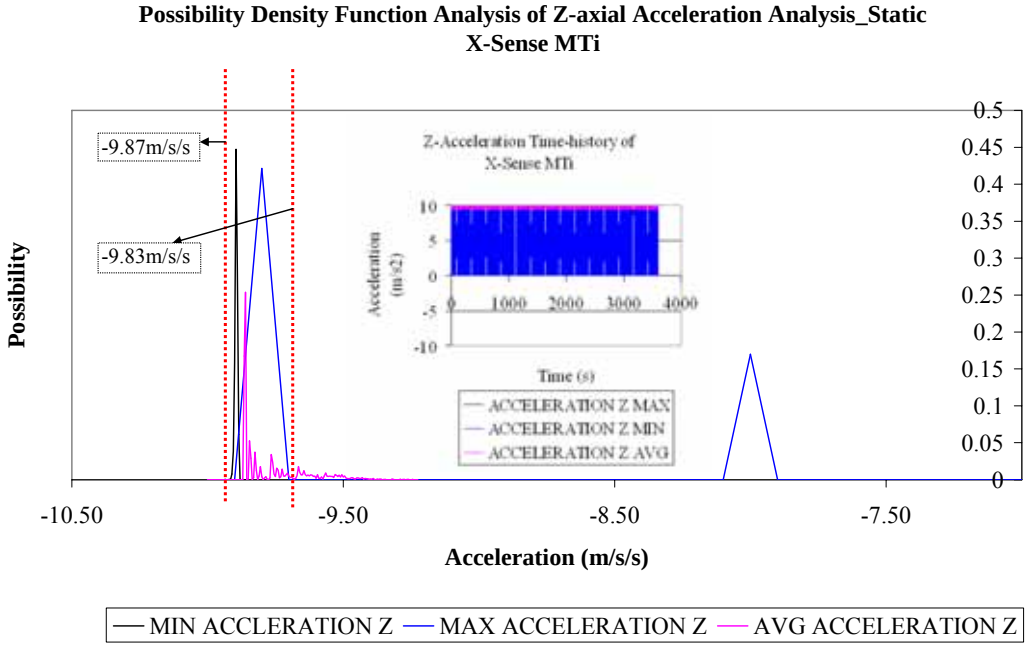

Figure 13: Possibility Density Function Analysis of Z-Acceleration_MTi (Static)

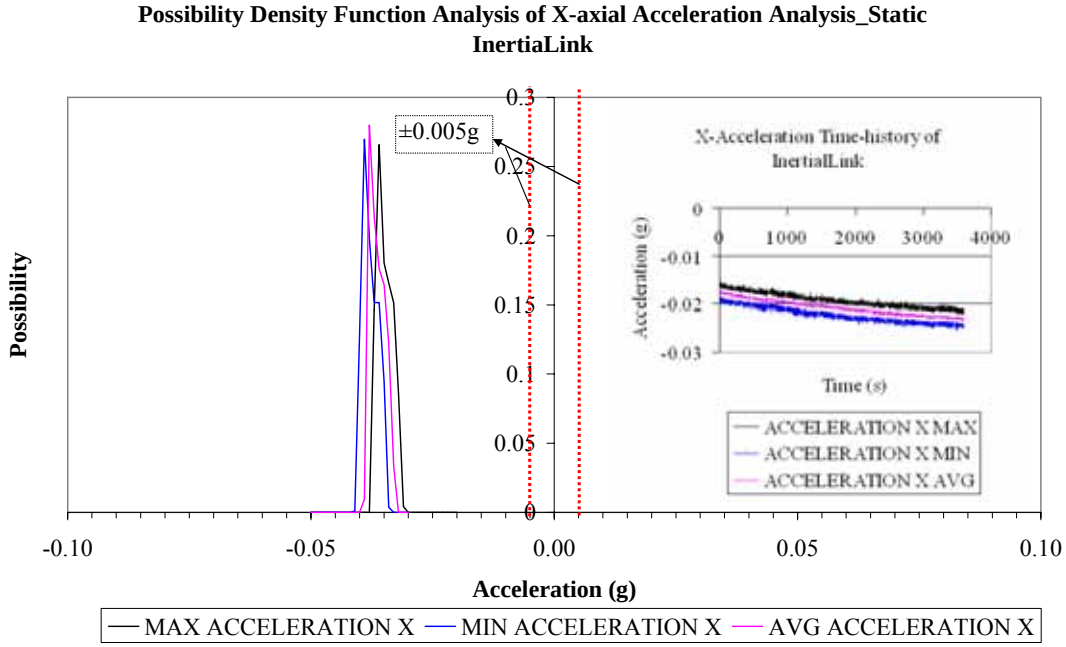

Figure 14: Possibility Density Function Analysis of X-Acceleration_InertiaLink (Static)

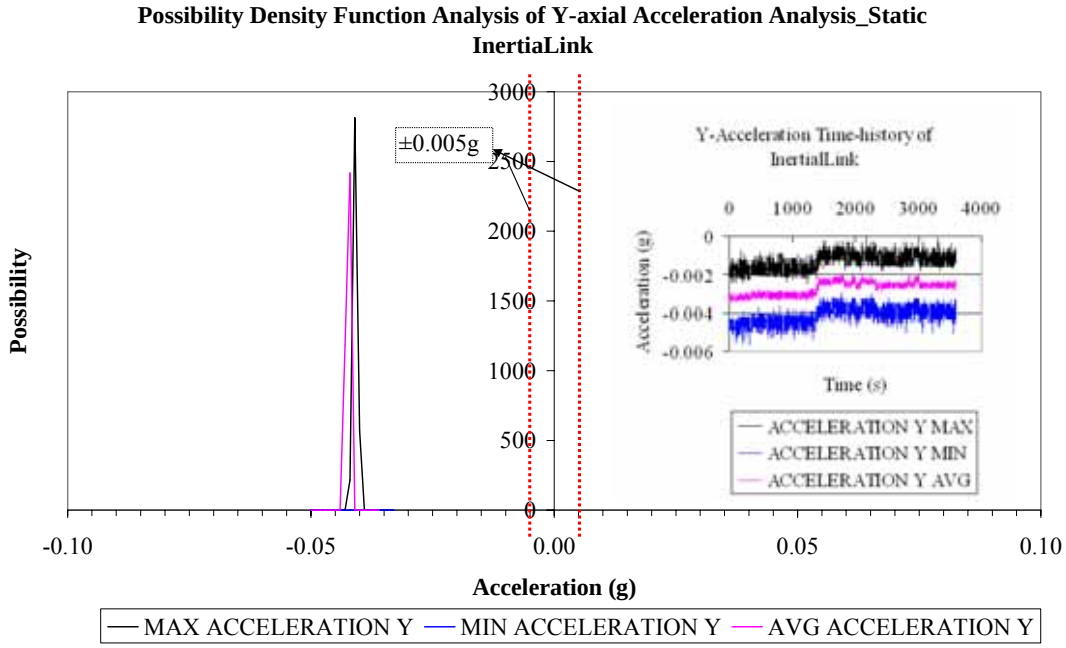

Figure 15: Possibility Density Function Analysis of Y-Acceleration_InertiaLink (Static)

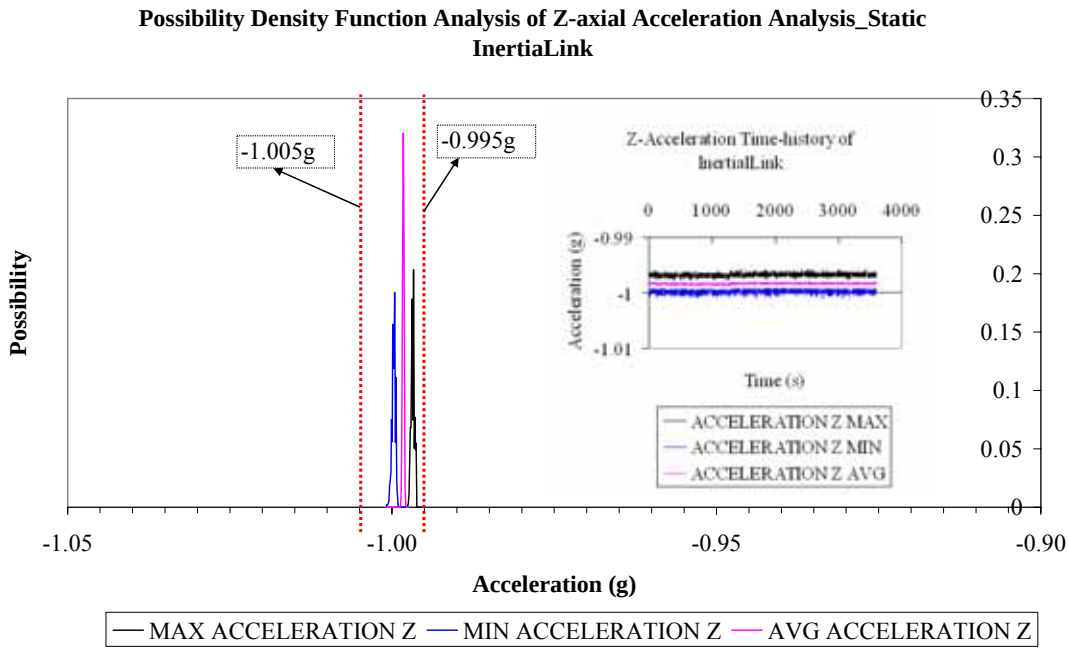

Figure 16: Possibility Density Function Analysis of Z-Acceleration_InertiaLink (Static)

3.2 Vibration Test

Figure 17, 19, 21, and 23 show the comparisons of displacement-time histories analysed from the measurement by the 4 different sensors. They were achieved by doing Fast Fourier Transform (FFT) to the original acceleration-time history records. The selected frequencies are 1Hz, 3Hz, 5Hz, and 10Hz, respectively. Under each frequency, the power spectrum density analysis for every sensor was also conducted so that the reliability of the data captured within different ranges of frequencies can be identified (Figure 18, 20, 22, 24).

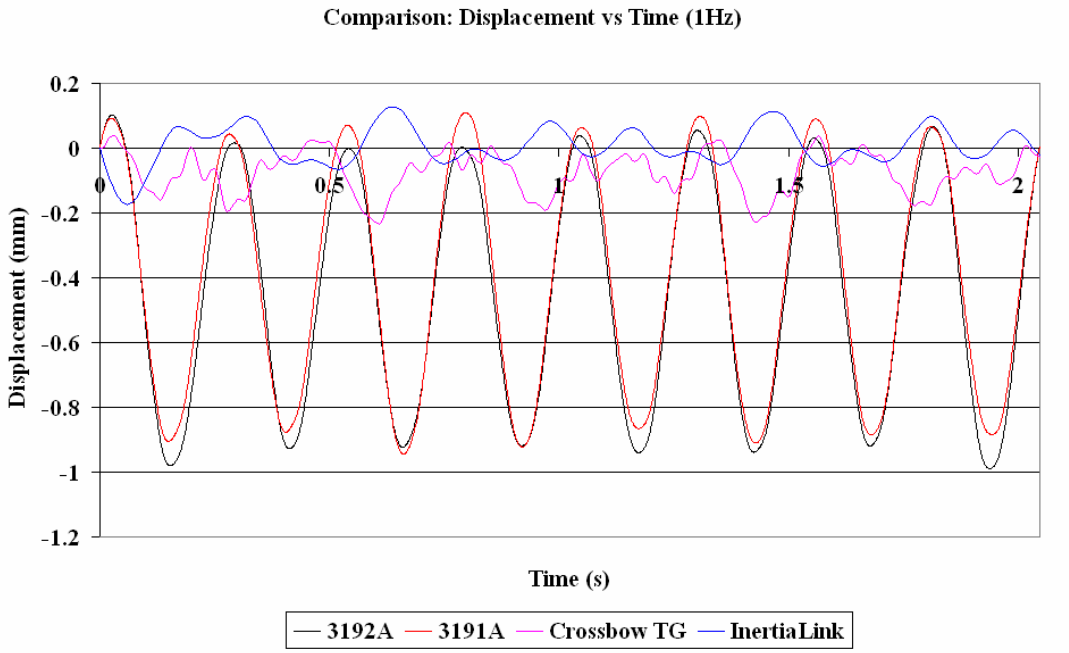

Figure 17: Analysis of Displacement-time Histories at 1Hz

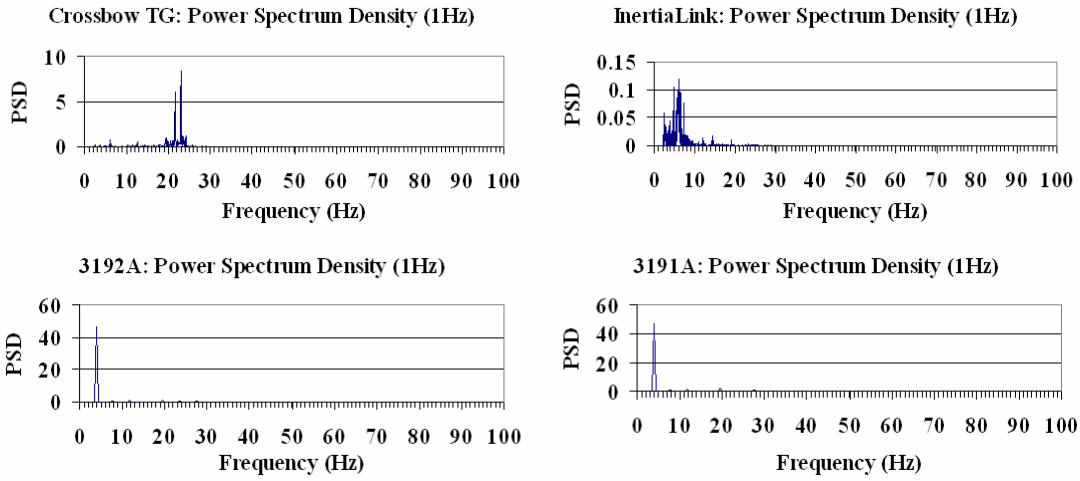

Figure 18: Power Spectrum Density Analysis at 1Hz

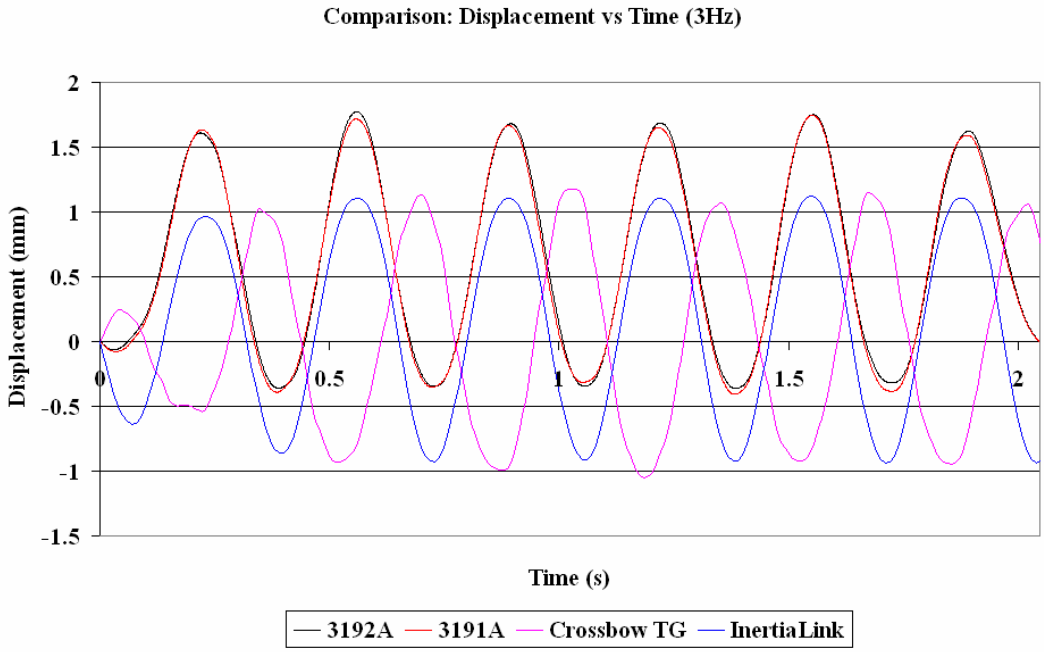

Figure 19: Analysis of Displacement-Time Histories at 3Hz

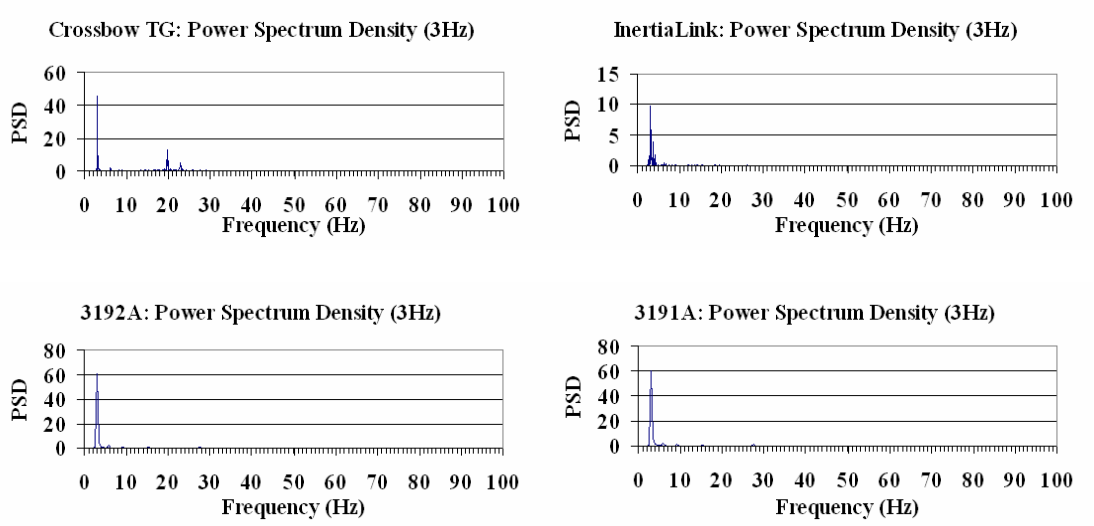

Figure 20: Power Spectrum Density Analysis at 3Hz

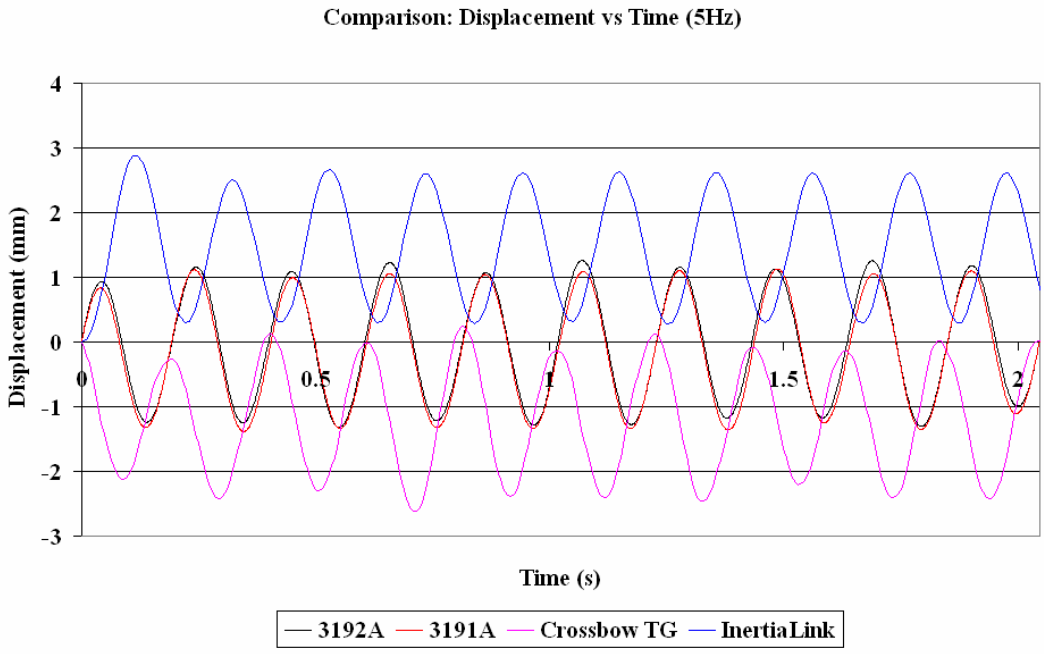

Figure 21: Analysis of Displacement-Time Histories at 5Hz

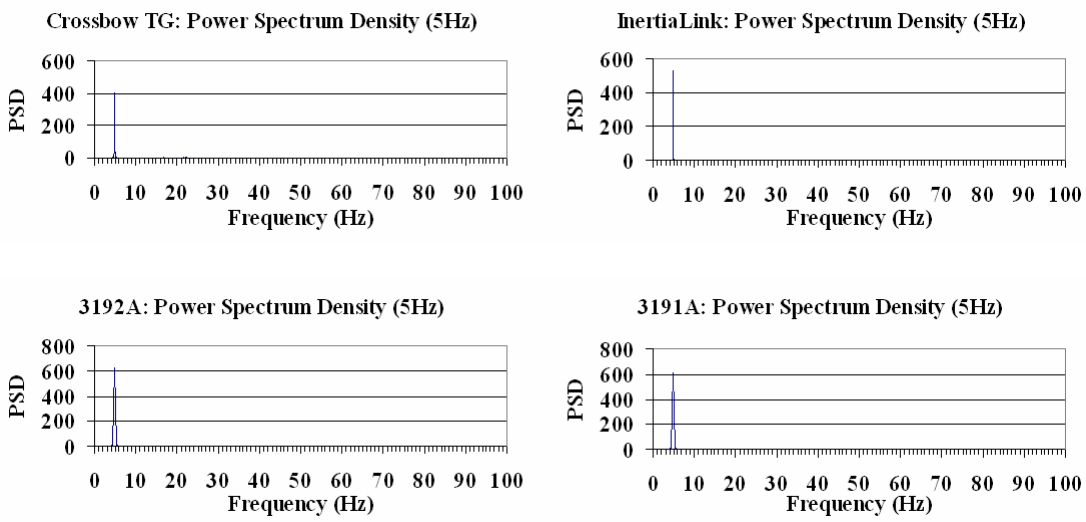

Figure 22: Power Spectrum Density Analysis at 5Hz

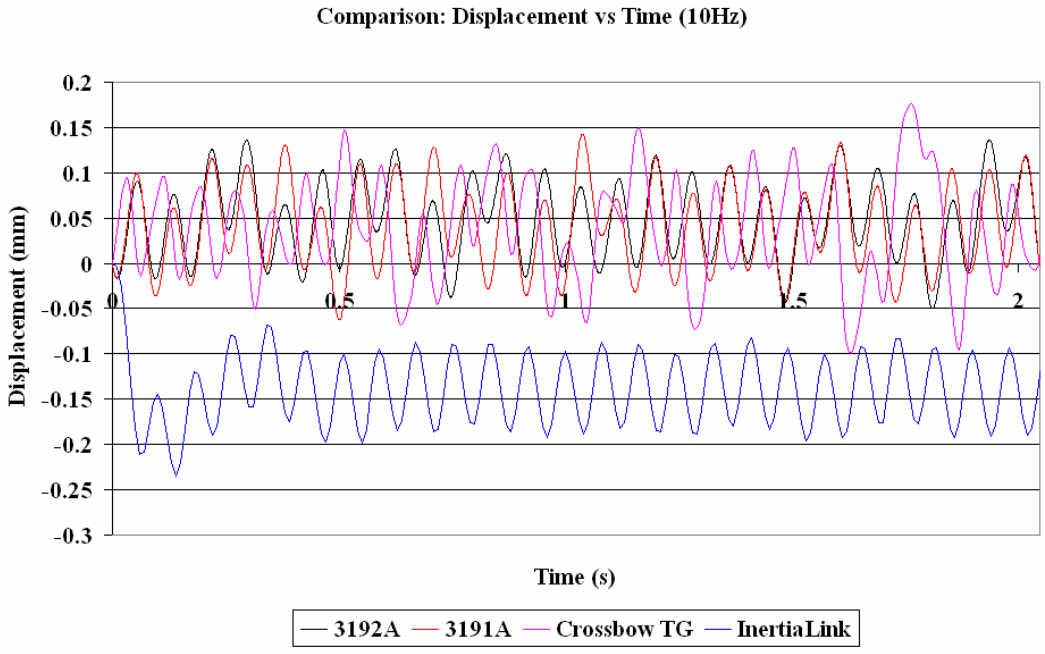

Figure 23: Analysis of Displacement-Time Histories at 10Hz

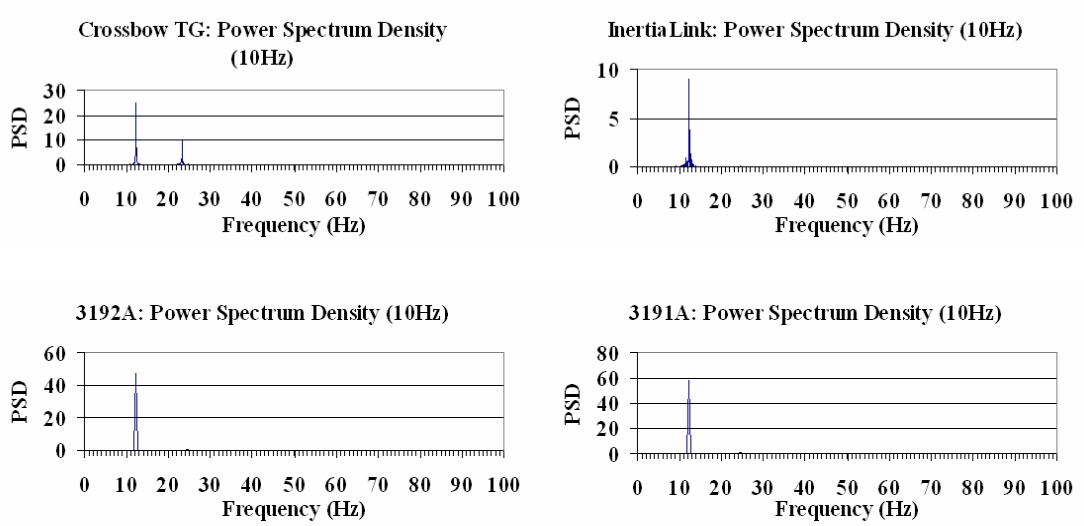

Figure 24: Power Spectrum Density Analysis at 1Hz

4. Discussion

A summary of the performance of the different sensors is presented in Table 2.

No	Sensor	Measurement	Accuracy / Reliability		
			Static	Vibration (<3Hz)	Vibration (≥3Hz)
1	Crista_IMU	X- Axial Acceleration	?	--	--
		Y- Axial Acceleration	N	--	--
		Z-Axial Acceleration	Y	--	--
2	Crossbow TG	X- Axial Acceleration	N	N	Y
		Y- Axial Acceleration	N	N	Y
		Z-Axial Acceleration	N	N	Y
3	X-Sens MTi	X- Axial Acceleration	Y	--	--
		Y- Axial Acceleration	N	--	--
		Z-Axial Acceleration	Y	--	--
4	InertiaLink	X- Axial Acceleration	N	N	Y
		Y- Axial Acceleration	N	N	Y
		Z-Axial Acceleration	Y	N	Y

Notes:
1. "Y" represents yes, which means the sensor can reach its advertised functions
2. "N" represents no, which means the sensor can reach its advertised functions
3. "–" means no comments
4. "?" means no conclusion

Table 2: Summary of performances of different sensors

4.1 Static test

From the results shown in the previous section, the following observations can be obtained for each of the sensors.

Crista_IMU: Figure 5 shows that even thought the lower boundary of the x-axial accelerations (down to -0.13 m/s^2) failed to squeeze into the error range (±1%, which is ±0.01 m/s^2) estimated by the manufacturer, some part of the upper limit (up to 0.1 m/s^2) was included in that error range. However, regarding the y-axial acceleration readings (Figure 6), the real measurements (0.68 m/s^2 to 0.84 m/s^2) are far beyond the error limits (±1%, which is ±0.01 m/s2). Comparing with the x- and y-axial performance, measurement along vertical direction (z-axial) revealed relatively higher accuracy. From Figure 7, it is clear that more than 95% of the readings are allocated within the designed error range (1%, which means from -9.903 m/s^2 to -9.706 m/s^2).

Crossbow_TG: From figure 8, it is clear that only the boundary drawn by the maximum value of x-axial accelerations was mostly allocated within the advertised error range (±0.085m/s^2) from the manufacturer. Moreover, the lower boundary drawn by the minimum accelerations of each second (down to -2.9 m/s^2) exceeded the "official" error limitations by more than three times. Regarding y-axial accelerations (Figure 9), both the upper boundary (up to 0.6m/s^2) and lower boundaries (down to2.95m/s^2) are beyond the manufacturer's specifications. Similarly, along z-axis (Figure 10), only the lower boundary fits in the error range (-1.0085g to -0.9915g) while the upper boundary is approximately 0.11g higher than it.

X-Sense MTi: Figure 11 shows the distribution of the x-axial accelerations of MTi. From the graph, even though both upper and lower boundaries are partly addressed beyond the error range (±0.02 m/s^2) defined in the specification sheet of the product, it is promising that for the most part the readings are within the range, which means that there is a certain reliability for x-axial measurement of the MTi in the static test. A similar situation occurred along z-axis, which has even better reliability in the readings according to Figure 13. However, for the y-axis, based on the graphs show in Figure 12, the reliability should be discounted because of the dispersive distribution of the readings (from 0 to 0.12 m/s^2).

InertiaLink: Figure 14, 15, and 16 show the distributions of accelerations along x-, y-, and z-axes respectively. It is clear that only z-axial accelerations are within the error range (-1.005g to -0.995g) from the sensor specifications. The x- and y- axes results (-0.04g~-0.03g and -0.45g~-0.39g, respectively) are not to be sufficiently accurate.

4.2 Vibration Test

Because of the synchronization difficulty, the displacement-time histories have different waves, either sine wave or cosine wave. However, the focus of the vibration tests is on the capabilities of those sensors to capture different motions at different frequencies, as well as the accuracy of the readings. In this case, only the period and the amplitude of the waves are of concern. From Figure 17, 19, 21, 23, it is obvious that the readings from the different sensors started to become consistent when the vibration was equal or higher than 3Hz. It is also worth noting that according to the power spectrum analysis (Figure 18, 20, 22, 24), when the input vibration exceeds 3Hz, both Crossbow_TG and InertiaLink are capable of capturing different level of frequencies with high accuracy.

5. Conclusion

From the above discussion, following conclusions can be drawn about those low-cost sensors:

1. The durability of those sensors is sufficient for most circumstances. Over 24 hours measurements were conducted and the data logging processes all went smoothly.

2. The accuracy of the records from those sensors varies as can be seen from Table 2.

3. The repeatability of the sensors is very satisfactory. The same test was repeated several times and the readings were identical.

4. The precision of those sensors in catching the motion of the object is reliable when the frequency of the object is above 3Hz.

REFERENCES

Allen J, Sacks E, (1998), Computer-Aided Micro-Mechanism Design, *ASME MEMS Symposium*, USA.

DARPA, (2007), http://www.arpa.mil/MTO/Programs/mems/index.html.

Cannon M.E, Schleppe J.B, McLellan J.F, Ollevier T, (1992), Real-time Heading Determination Using an Integrated GPS-Dead Reckoning System, *Proceedings of ION GPS-92*, Institute of Navigation, Washington, D.C., pp. 767-773.

McLellan J.F, (1992), Design and Analysis of a Low Cost GPS-Aided Navigation System, *MSc. Thesis*, 1996, Report No.20097.

Sheimy N, (2000), Integrated Systems and their Impact on the Future of Positioning, Navigation and Mapping Applications, *Proceedings Quo Vadis International Conference*, FIG Working Week, 2000, 21-26 May, Prague.